Received: 27 May 2021 | Revised: 28 November 2021 | Accepted: 8 December 2021

DOI: 10.1002/oa.3079

RESEARCH ARTICLE

Insights into the diagnostic efficacy and macroscopic appearance of endocranial bony changes indicative of tuberculous meningitis: Three example cases from the Robert J. Terry Anatomical Skeletal Collection

Olga Spekker[1] | David R. Hunt[2] | William Berthon[1,3] | Erika Molnár[1] | György Pálfi[1]

[1]Department of Biological Anthropology, University of Szeged, Szeged, Hungary

[2]Department of Anthropology, National Museum of Natural History, Smithsonian Institution, Washington, DC, USA

[3]Chaire d'Anthropologie Biologique Paul Broca, École Pratique des Hautes Études (EPHE), PSL University, Paris, France

Correspondence
Olga Spekker, Department of Biological Anthropology, University of Szeged, Közép fasor 52, H-6726 Szeged, Hungary.
Email: olga.spekker@gmail.com

Funding information
University of Szeged Open Access Fund, Grant/Award Number: 5626; Hungarian State Eötvös Fellowship 2016 of the Tempus Public Foundation, Grant/Award Number: 77466; NTP-NFTÖ-16 of the Hungarian Ministry of Human Capacities & Human Capacities Grant Management Office, Grant/Award Number: 1116; National Research, Development and Innovation Office (Hungary), Grant/Award Number: K 125561

Abstract

Recently, the combined macroscopic and statistical evaluation of 427 identified pre-antibiotic era skeletons from the Terry Collection (Washington, DC, USA) revealed that there is a positive association between tuberculous meningitis (TBM) and four endocranial alteration types, namely, granular impressions (GIs), abnormal blood vessel impressions (ABVIs), periosteal appositions (PAs), and abnormally pronounced digital impressions (APDIs). Although all the four lesion types can be used as diagnostic criteria for TBM in the paleopathological practice, they do not have the same diagnostic value. The first aim of the current paper is to further highlight the diagnostic value of GIs, ABVIs, PAs, and APDIs by calculating and discussing their diagnostic sensitivity and specificity estimate values, as well as their association with each other from the 427 identified pre-antibiotic era skeletons of the Terry Collection. The second aim is to demonstrate three example cases from the Terry Collection, who exhibit bony changes on the inner skull surface that are representative of the macromorphological appearance and co-occurrence of GIs, ABVIs, PAs, and APDIs (in different combinations). Based on the generated sensitivity and specificity estimate values, GIs are sufficient enough on their own to make a definitive diagnosis of TBM, whereas ABVIs, PAs, and APDIs are not specific to the disease but can be of tuberculous origin. The χ^2 test results regarding the association of ABVIs, PAs, and APDIs revealed that their co-occurrence with each other (in any possible combination) is significantly more common in individuals who died of TB than in those who died of non-TB causes—it implies that the chance of them being tuberculous in origin is higher when they simultaneously occur with each other. The three cases demonstrated in detail in the paper provide paleopathologists with a stronger basis for identifying TBM in ancient human remains that reveal endocranial alterations resembling that of the presented cases.

Erika Molnár and György Pálfi shared last authors.

KEYWORDS
abnormal blood vessel impressions, abnormally pronounced digital impressions, diagnostic sensitivity, diagnostic specificity, granular impressions, identified pre-antibiotic era skeletons, paleopathological diagnosis, periosteal appositions

1 | INTRODUCTION

The paleopathological diagnosis of tuberculosis (TB) essentially relies on the identification of macroscopic lesions in the human skeleton that have been found to be associated with different forms of the disease (e.g., pulmonary TB/TB pleurisy, tuberculous meningitis [TBM], and skeletal TB) (Mariotti et al., 2015; Santos & Roberts, 2006). Among these macroscopic bony changes, there are four endocranial alteration types, that is, granular impressions (GIs) (Figure 1a), abnormal blood vessel impressions (ABVIs) (Figure 1d), periosteal appositions (PAs) (Figure 1c), and abnormally pronounced digital impressions (APDIs) (Figure 1b), which have been considered as indicative of TBM (Schultz, 2001, 2003; Spekker, 2018; Spekker, Hunt, et al., 2020; Spekker, Schultz, et al., 2020; Spekker et al., 2021). The most important information regarding the four aforementioned lesion types (i.e., macromorphology, common localizations, pathophysiology, and associated etiologies) is summarized in Table 1.

Although GIs, ABVIs, PAs, and APDIs were used as diagnostic criteria for TBM in a number of paleopathological studies on osteoarchaeological series (e.g., Abegg et al., 2020; Jankauskas, 1999; Lei et al., 2019; Teschler-Nicola et al., 2015) since the late 20th century, their diagnostic value has been questioned (Janovic et al., 2015; Lewis, 2004; Roberts et al., 2009). As part of a comprehensive research project (Spekker, 2018), 427 human pre-antibiotic era skeletons from the Robert J. Terry Anatomical Skeletal Collection (Department of Anthropology, National Museum of Natural History, Smithsonian Institution, Washington, DC, USA) were analyzed to evaluate the diagnostic value of the four endocranial alteration types indicative of TBM (i.e., GIs, ABVIs, PAs, and APDIs)—234 individuals who died of TB (TB group) and 193 individuals who died of non-TB causes (NTB group) (Table S1).

The findings revealed some differences in the frequency of GIs, ABVIs, PAs, and APDIs, as well as their co-occurrence with each other and with non-endocranial bony changes likely associated with TB, especially in consideration of the cause of death of individuals. The generated frequency data are briefly summarized in Table 2 (see in detail in Spekker, 2018; Spekker, Hunt, et al., 2020; Spekker, Schultz, et al., 2020; Spekker et al., 2021). A total of 62.06% (265/427) of the analyzed individuals exhibited at least one endocranial alteration type, with APDIs being the most frequently registered (216/427, 50.59%), and GIs, ABVIs, and PAs occurring in similar proportions (74/427, 17.33%; 62/427, 14.52%; and 67/427, 15.69%, respectively)

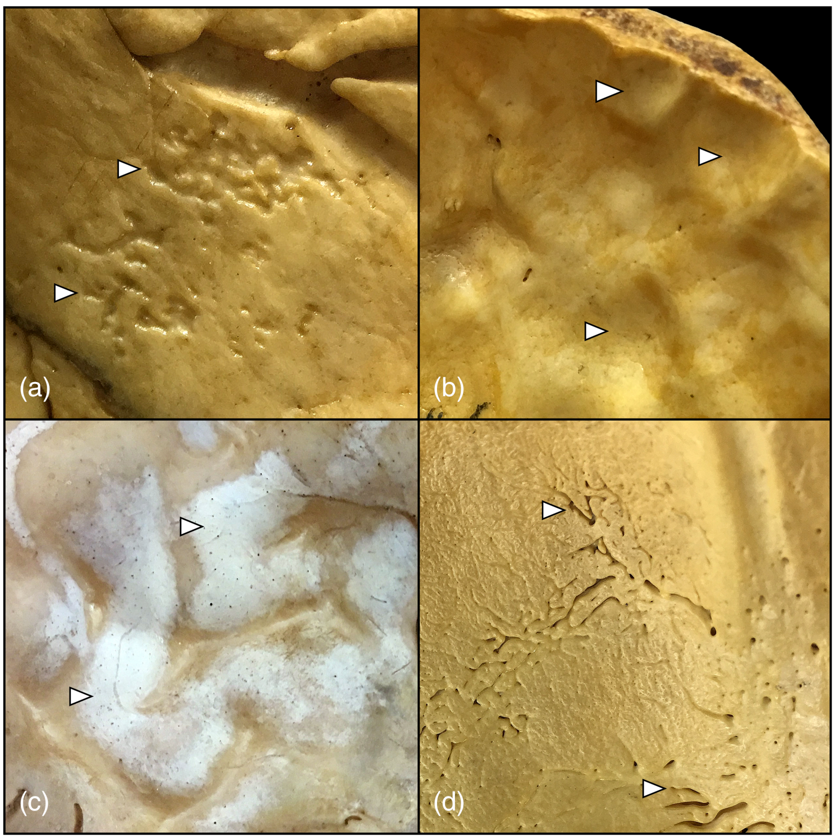

FIGURE 1 Close-up of the four different endocranial alteration types indicative of tuberculous meningitis (white arrows): (a) GIs (Terry No. 522, 30-year-old, male, died of pulmonary TB), (b) APDIs (Terry No. 466, 31-year-old, male, died of pulmonary TB), (c) PAs (Terry No. 1300, 28-year-old, male, died of TB), and (d) ABVIs (Terry No. 329, 18-year-old, male, died of pulmonary TB) [Colour figure can be viewed at wileyonlinelibrary.com]

TABLE 1 Endocranial alteration types indicative of TBM

Lesion type	Macromorphology	Common localizations	Pathophysiology	Associated etiologies
Granular impressions (GIs) (Schultz, 1999, 2001, 2003; Schultz & Schmidt-Schultz, 2015; Spekker, Schultz, et al., 2020)	Small (0.5–1.0 mm in diameter), relatively shallow (less than 0.5 mm in depth), roundish impressions with smooth margins and walls that generally appear as isolated or confluent lesions grouped in clusters on the endocranial surface	Orbital part of the frontal bone, greater wings of the sphenoid bone, and squamous part of the occipital and temporal bones	Can be established by pressure atrophy of the tubercles formed on the outermost meningeal layer during later stages of TBM	TBM
Abnormal blood vessel impressions (ABVIs) (Schultz, 1993, 2001, 2003; Spekker, Hunt, et al., 2020)	Small, patch-like areas of very short, sinuous, branching blood vessel impressions on the endocranial surface—the aggregation of ABVIs can become extensive and net-like over time	Most protruding parts of the frontal and parietal bones, and along the sulci of the dural venous sinuses (particularly along the sulci of the sagittal and transverse sinuses)	Can develop secondary to the formation of an epidural hematoma	e.g., TBM, bacterial meningitis, trauma, and scurvy
Periosteal appositions (PAs) (Schultz, 1993, 2001, 2003; Spekker, Hunt, et al., 2020)	Hemorrhagic meningeal process: appositions of newly formed bone with a fibrous, porous, irregular, scab-like appearance—PAs can have a very smooth, more mature appearance over time Inflammatory meningeal process: small, flat, plate-like appositions of newly built bone—the isolated plates of PAs can become confluent as one or more layers, their contours become indistinct, and their plate-like character will be lost over time	Most protruding parts of the frontal and parietal bones, and along the sulci of the dural venous sinuses (particularly along the sulci of the sagittal and transverse sinuses)	Can be the result of the hemorrhagic and/or inflammatory processes of the meninges (the inflammatory, hemorrhagic, and mixed forms of PAs can be confused by macroscopic examinations only, but can be differentiated by microscopic investigations)	e.g., TBM, bacterial meningitis, trauma, and scurvy
Abnormally pronounced digital impressions (APDIs) (Schüller, 1940–1941; du Boulay, 1956; Burkhardt & Fischer, 1970; Bell, 1978; Schultz, 1993, 2001, 2003; Mahomed et al., 2012; Paul et al., 2013, 2014; Desai et al., 2014; Pemmaiah, 2015; Spekker et al., 2021)	Abnormally pronounced endocranial depressions, resembling finger imprints, that correspond to the cerebral gyri and are incompletely separated from each other by bony ridges of different sizes that match in their position to the cerebral sulci	Very slight stage: skullcap—squamous part of the frontal bone slight stage: skullcap—parietal bones and squamous part of the frontal bone pronounced stage: all over the skullcap and skull base	Can develop secondary to a prolonged rise in the intracranial pressure—the localized pressure exerted by the brain and its pulsating blood vessels on the underlying endocranial surface induces pressure atrophy of the bone	e.g., TBM and other central nervous system infections, trauma, brain tumors, and hemorrhages

(Spekker, 2018). The co-occurrence of at least two of the aforementioned endocranial alteration types was recorded in 26.00% (111/427) of the examined individuals, with two-thirds of the skeletons presenting two lesion types (72/111, 64.86%) (Spekker, 2018).

Of the 265 individuals that exhibited at least one endocranial alteration type indicative of TBM, about two thirds (167/265, 63.02%) revealed non-endocranial bony changes probably related to TB, such as periosteal new bone formations (PNBFs) on the visceral surface of

TABLE 2 Sensitivity and specificity estimate values for GIs, ABVIs, PAs, and APDIs

Terry collection ($N = 427$)	GIs (Spekker, Schultz, et al., 2020) TB group ($N_{TB} = 234$)	GIs NTB group ($N_{NTB} = 193$)	ABVIs (Spekker, Hunt, et al., 2020) TB group ($N_{TB} = 234$)	ABVIs NTB group ($N_{NTB} = 193$)	PAs (Spekker, Hunt, et al., 2020) TB group ($N_{TB} = 234$)	PAs NTB group ($N_{NTB} = 193$)	APDIs (Spekker et al., 2021) TB group ($N_{TB} = 234$)	APDIs NTB group ($N_{NTB} = 193$)
Number of individuals affected by the lesions	68 (i.e., TP)	6 (i.e., FP)	50 (i.e., TP)	12 (i.e., FP)	47 (i.e., TP)	20 (i.e., FP)	154 (i.e., TP)	62 (i.e., FP)
Number of individuals not affected by the lesions	166 (i.e., FN)	187 (i.e., TN)	184 (i.e., FN)	181 (i.e., TN)	187 (i.e., FN)	173 (i.e., TN)	80 (i.e., FN)	131 (i.e., TN)
Sensitivity (TP/N_{TB})	68/234 = 0.2906 (29.06%)		50/234 = 0.2137 (21.37%)		47/234 = 0.2009 (20.09%)		154/234 = 0.6581 (65.81%)	
1 − Sensitivity	0.7094 (70.94%)		0.7863 (78.63%)		0.7991 (79.91%)		0.3419 (34.19%)	
Specificity (TN/N_{NTB})	187/193 = 0.9689 (96.89%)		181/193 = 0.9378 (93.78%)		173/193 = 0.8964 (89.64%)		131/193 = 0.6788 (67.88%)	
1 − Specificity	0.0311 (3.11%)		0.0622 (6.22%)		0.1036 (10.36%)		0.3212 (32.12%)	
Sensitivity + specificity	0.7405		0.8485		0.9027		1.3369	

Note: Results regarding APDIs were already published in Spekker et al. (2021).
Abbreviations: FN, false negatives; FP, false positives; TP, true positives; TN, true negatives.

the ribs (117/265, 44.15%) and signs of hypervascularization on the anterior and/or lateral aspects of the vertebral bodies (115/265; 43.40%) (Spekker, 2018). Two thirds of the skeletons with at least one endocranial alteration type indicative of TBM (106/167, 63.47%) simultaneously presented at least two different non-endocranial lesion types (Spekker, 2018).

The frequency of GIs, ABVIs, PAs, and APDIs, as well as their co-occurrence with each other and with non-endocranial bony changes likely associated with TB, was higher in the TB group when compared with the NTB group. APDIs and PAs occurred about twice as often (65.81% [154/234] vs. 32.12% [62/193] and 20.09% [47/234] vs. 10.36% [20/193], respectively), whereas ABVIs and GIs occurred about three and a half times (21.37% [50/234] vs. 6.22% [12/193]) and 10 times (29.06% [68/234] vs. 3.11% [6/193]) often, respectively (Table 2) (Spekker, 2018; Spekker, Hunt, et al., 2020; Spekker, Schultz, et al., 2020; Spekker et al., 2021). In addition, the co-occurrence of at least two of the aforementioned endocranial alteration types was about five times more common in the TB group (41.03% [96/234] vs. 7.77% [15/193]), with 58 (60.42%), 34 (35.41%), and four (4.17%) individuals exhibiting two, three, and four lesion types, respectively (Spekker, 2018). In the NTB group, two endocranial alteration types were concurrently present in the majority of the skeletons (14/15, 93.33%)—only one individual revealed three lesion types (Spekker, 2018). Finally, the co-occurrence of at least one endocranial alteration type and at least one non-endocranial alteration type was about three times more common in the TB group (80.11% [145/181] vs. 26.19% [22/84]), with 61.33% (111/181) of the skeletons exhibiting costal PNBFs and 56.35% (102/181) of the skeletons presenting signs of vertebral hypervascularization (Spekker, 2018).

The χ^2 analysis of the frequency data revealed that GIs, ABVIs, PAs, and APDIs were significantly more common in the TB group than in the NTB group (Spekker, 2018; Spekker, Hunt, et al., 2020; Spekker, Schultz, et al., 2020; Spekker et al., 2021). These results imply that there is a positive association between TB and the four examined endocranial alteration types; thus, all of them can be used as diagnostic criteria for the disease in the paleopathological practice. However, based on our findings (Spekker, 2018; Spekker, Hunt, et al., 2020; Spekker, Schultz, et al., 2020; Spekker et al., 2021), it also seems obvious that GIs, ABVIs, PAs, and APDIs do not have the same diagnostic value in the identification of TB in ancient human remains. The diagnostic efficacy of each aforementioned lesion type (i.e., the ability of them to separate individuals who have TB from those who do not have the disease) can be expressed by two diagnostic probability measures, namely sensitivity (i.e., the probability of presenting GIs, ABVIs, PAs, or APDIs given that the individual actually suffered from TB) and specificity (i.e., the probability of not having GIs, ABVIs, PAs, or APDIs given that the individual did not suffer from TB) (Boldsen, 2001; Dangvard Pedersen et al., 2019; Milner & Boldsen, 2017).

In a previous study, Spekker et al. (2021) revealed that the sensitivity of APDIs (i.e., 0.6581) is more than one minus the specificity of APDIs (i.e., 0.3212) (Table 2). Similar to the χ^2 test results, it indicates that there is a positive association between APDIs and TB (Spekker et al., 2021). It also means that the probability of having this endocranial alteration type is higher in individuals with TB than in those without the disease but does not imply that the majority of individuals with APDIs actually suffer from TB (Spekker et al., 2021). Based on the rather high sensitivity estimate value (i.e., 0.6581), APDIs are suitable for screening purposes even if not all TB cases can be recognized with their application as diagnostic criteria (Spekker et al., 2021). It also seems obvious that based on the rather low specificity estimate value (i.e., 0.6788), APDIs are not sufficient on their own to make a definitive diagnosis of TB, as this lesion type is not specific to the disease (Spekker et al., 2021). These results are not surprising if we consider that APDIs can develop only in case of meningeal involvement, which is not present in all patients with TB, and besides TBM, numerous medical conditions, for example, trauma, brain tumors, and hemorrhages, can result in the formation of APDIs on the inner skull surface (Myers, 2007; Paul et al., 2013, 2014).

Taking into account our previous findings, the main aim of the current paper is to further highlight the diagnostic value of the four endocranial alteration types indicative of TBM (i.e., GIs, ABVIs, PAs, and APDIs) by calculating and discussing the diagnostic sensitivity and specificity estimate values of GIs, ABVIs, and PAs (as stated above, these diagnostic probability measures for APDIs were already presented in detail in Spekker et al., 2021), as well as the association of the four endocranial alteration types with each other, using the frequency data of our previously published studies (Table 2) (Spekker, 2018; Spekker, Hunt, et al., 2020; Spekker, Schultz, et al., 2020; Spekker et al., 2021).

Similar to the meticulous medical descriptions from the pre-antibiotic era, detailed documented case studies with TB as the cause of death from the same time period also provide a unique insight into the natural history and different manifestations of TB. They help us in identifying non-pathognomonic bony changes and/or patterns of lesions that can later be used as diagnostic criteria for TB in the paleopathological practice. Nonetheless, only a few detailed documented pre-antibiotic era case studies presenting TBM-related endocranial alterations (e.g., Maczel, 2003; Ortner, 2003; Pálfi et al., 2012; Schultz & Schmidt-Schultz, 2015) have been published in the paleopathological literature until now.

To fulfill this lack, in the current paper, we demonstrate three example cases from the Terry Collection (i.e., Terry No. 562, Terry No. 933R, and Terry No. 1159). These three cases exhibit bony changes on the inner surface of the skull that are representative of the macromorphological appearance (e.g., localization) and co-occurrence of GIs, ABVIs, PAs, and APDIs (in different combinations). Besides the endocranial alterations indicative of TBM, the three demonstrated cases also present different types of non-endocranial bony changes that can be related to TB (e.g., costal PNBFs and sings of vertebral hypervascularization).

2 | MATERIAL AND METHODS

The examined skeletal material, and the applied macromorphological and statistical methods have been discussed in detail in previous papers (Spekker, 2018; Spekker, Hunt, et al., 2020; Spekker, Schultz, et al., 2020; Spekker et al., 2021); therefore, only a brief summary of this information is presented here. The skeletal material consisted of 427 human pre-antibiotic era skeletons from the Terry Collection: 234 individuals with TB as the cause of death (TB group; 169 males and 65 females) and 193 individuals with non-TB causes of death (NTB group; 106 males and 87 females) (Table S1). In both groups, the selected skeletons were assessed for the presence, macroscopic characteristics, and co-occurrence of different types of endocranial and non-endocranial bony changes probably related to TB. Following the macromorphological investigation, absolute and percentage frequencies of GIs, ABVIs, PAs, and APDIs, as well as their co-occurrence with each other and with non-endocranial skeletal lesions likely associated with TB were calculated in both the TB group and NTB group, and then, the significance of difference in the frequencies between the two groups was determined by χ^2 testing.

In the current study, diagnostic sensitivity and specificity estimate values for GIs, ABVIs, and PAs were generated, using the MedCalc statistical software package. Furthermore, to determine the significance of difference in the frequencies of the co-occurrence of ABVIs, PAs, and APDIs with each other (in any possible combination) between the TB group and the NTB group, χ^2 testing was undertaken, using the R statistical software package. Finally, to present the most characteristic macroscopic features of GIs, ABVIs, PAs, and APDIs (i.e., localization, extent, number, and prominence), as well as their co-occurrence with each other (in different combinations), three cases were selected from the TB group for discussion in detail. The three demonstrated individuals from the Terry Collection are the following:

- Terry No. 562: a 17-year-old (1911/1912–1929) female recorded to have died of pulmonary TB. The skeleton is well-preserved and complete;
- Terry No. 933R: a 40-year-old (1903–1943) male who probably died of peritoneal TB without involvement of the lungs. The skeleton is well-preserved and complete; and
- Terry No. 1159: a 26-year-old (1911–1937) male whose morgue record states pulmonary TB as the cause of death. The skeleton is well-preserved and complete.

3 | RESULTS AND DISCUSSION

3.1 | Diagnostic efficacy

The generated sensitivity and specificity estimate values for the four endocranial alteration types indicative of TBM can be seen in Table 2. Similar to the previously published χ^2 test results (Spekker, Hunt, et al., 2020; Spekker, Schultz, et al., 2020), the calculated sensitivity and specificity estimate values for GIs, ABVIs, and PAs support that there is a positive association between the aforementioned lesion types and TB, as their sensitivity is more than one minus their specificity (Table 2) (Boldsen, 2001; Dangvard Pedersen et al., 2019). It also means that the probability of presenting GIs, ABVIs or PAs is higher in individuals with TB than in those without TB.

As for the sensitivity estimate values (Table 2), if GIs, ABVIs, or PAs are present on the inner skull surface, there is a 29.06%, 21.37% or 20.09% probability of a true TB diagnosis, respectively. On the one hand, the findings (Table 2) indicate that GIs, ABVIs, and PAs cannot be used to identify a large number of TB cases due to the rather high false negative rates (i.e., 0.7094, 0.7863, and 0.7991, respectively); therefore, these lesion types are not suitable for screening purposes. In contrast to GIs, ABVIs, and PAs, the sensitivity of APDIs is rather high (i.e., 0.6581); meaning that with the application of APDIs as diagnostic criteria, quite a large number of individuals with TB can be recognized (Spekker et al., 2021). Nevertheless, it should not be expected that any of the four examined endocranial alteration types could be used to identify all individuals with TB, as they can develop only in case of meningeal involvement (i.e., TBM) that is a very rare form of TB, occurring in less than 1% of the active TB cases today (Myers, 2007).

On the other hand, the results (Table 2) suggest that GIs can be considered as specific signs of TB due to the extremely low false positive rate (i.e., 0.0311); consequently, GIs are sufficient enough on their own to make a definitive diagnosis of TBM. It is not surprising if we consider that GIs are defined as endocranial impressions established by pressure atrophy of the tubercles (formed on the outermost

TABLE 3 Results of the χ^2 tests regarding the co-occurrence of ABVIs, PAs, and APDIs with each other (in all possible combinations)

	ABVIs + PAs		ABVIs + APDIs		PAs + APDIs		ABVIs + PAs + APDIs	
Terry collection ($N = 427$)	**TB group ($N_{TB} = 234$)**	**NTB group ($N_{NTB} = 193$)**	**TB group ($N_{TB} = 234$)**	**NTB group ($N_{NTB} = 193$)**	**TB group ($N_{TB} = 234$)**	**NTB group ($N_{NTB} = 193$)**	**TB group ($N_{TB} = 234$)**	**NTB group ($N_{NTB} = 193$)**
Number of individuals affected by the combination of lesions	24 (10.26%)	2 (1.04%)	36 (15.38%)	3 (1.55%)	43 (18.38%)	7 (3.63%)	20 (8.55%)	0 (0.00%)
Number of individuals not affected by the combination of lesions	210 (89.74%)	191 (98.96%)	198 (84.62%)	190 (98.45%)	191 (81.62%)	186 (96.37%)	214 (91.45%)	193 (100.00%)
Results of the χ^2 tests	$\chi^2 = 15.724$ df = 1 $P < 0.001$		$\chi^2 = 24.376$ df = 1 $P < 0.001$		$\chi^2 = 22.255$ df = 1 $P < 0.001$		$\chi^2 = 17.306$ df = 1 $P < 0.001$	

Note: Individual data were already published in Spekker, Hunt, et al. (2020), Spekker, Schultz, et al. (2020), and Spekker et al. (2021).

TABLE 4 Registered TB-related bony changes in the three skeletons described in detail (+ = present; − = not present)

Registered bony changes	Terry no. 562	Terry no. 933R	Terry no. 1159
Endocranial alterations			
Abnormally pronounced digital impressions	+ (frontal & parietals)	+ (frontal)	+ (skullcap & skull base)
Abnormal blood vessel impressions	–	+ (frontal)	–
Periosteal appositions	–	–	+ (frontal, parietals, temporals, & occipital)
Granular impressions	+ (frontal, temporals, sphenoid, & occipital)	+ (frontal, parietals, temporals, sphenoid, & occipital)	+ (frontal & occipital)
Nonendocranial alterations			
Signs of vertebral hypervascularization	+ (T9–12 & L1–5)	+ (C6–7, T1–12, & L1–2)	+ (T1–12 & L1–3)
Periosteal new bone formations on the visceral rib surface	+ (left 2nd–6th ribs)	+ (right 11th rib)	+ (left 2nd–11th ribs)
Signs of diffuse, symmetrical periostitis	–	–	+ (tibiae, humeri, & right scapula)

meningeal layer) that are the hallmark features of TB (Schultz, 1993, 1999, 2001, 2003; Schultz & Schmidt-Schultz, 2015; Spekker, Schultz, et al., 2020). Although in case of ABVIs and PAs (Table 2), the generated false positive rates are quite low (i.e., 0.0622 and 0.1036, respectively), they are not sufficient enough on their own to make a definitive diagnosis of TBM, since besides TBM, other medical conditions can also result in the development of ABVIs and PAs (Schultz, 1993, 1999, 2001, 2003; Schultz & Schmidt-Schultz, 2015; Spekker, Hunt, et al., 2020). It should be mentioned that similar to ABVIs and PAs, APDIs are not specific to TBM (Table 2)—among the four evaluated endocranial alteration types, APDIs had the lowest

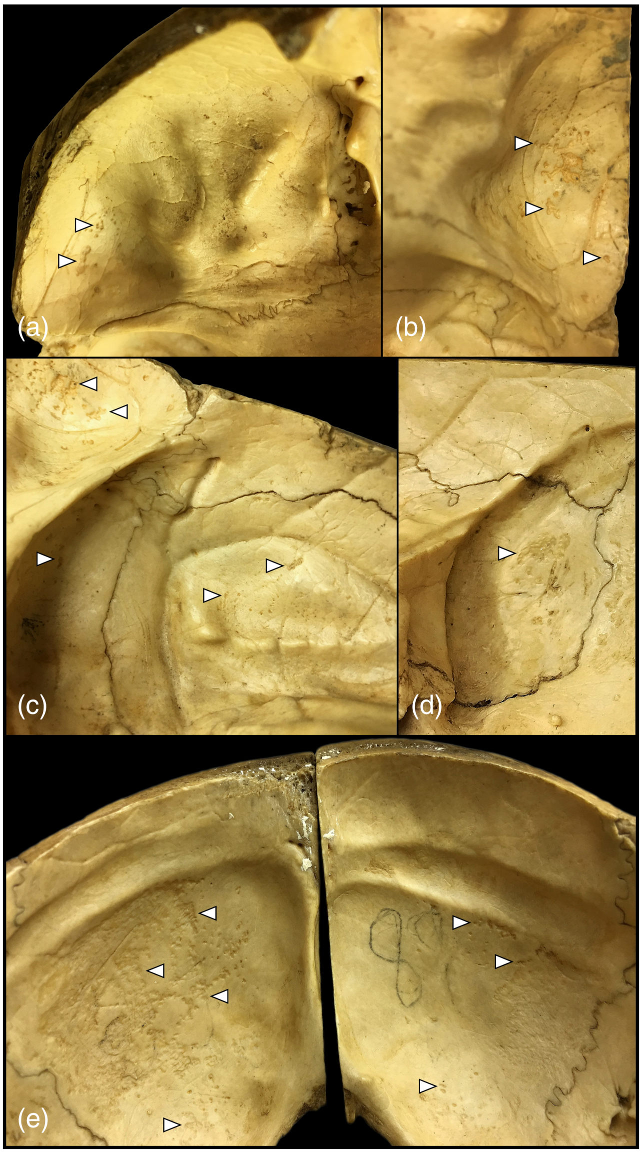

FIGURE 2 GIs (white arrows) on the (a) left side and (b) right side of the orbital part of the frontal bone, (c) the right greater wing of the sphenoid bone and the squamous part of the right temporal bone, (d) the petrous part of the right temporal bone, and (e) the squamous part of the occipital bone of Terry No. 562 (17-yearold, female, died of pulmonary TB) [Colour figure can be viewed at wileyonlinelibrary.com]

specificity estimate value (i.e., 0.6788) (Spekker et al., 2021). Assumed from the above, the paleopathological diagnosis of TBM cannot be established based only on the presence of ABVIs, PAs or APDIs on the inner skull surface.

The χ^2 test results regarding the association of ABVIs, PAs, and APDIs (Table 3) revealed that their co-occurrence with each other (in any possible combination) is significantly more common in individuals who died of TB than in those who died of non-TB causes. This implies that in cases where these lesions concomitantly occur with each other, the chance of them being tuberculous in origin is higher than in cases where they are present alone. Although the co-occurrence of ABVIs, PAs, and/or APDIs on the endocranial surface without the simultaneous presence of GIs is still not enough to make a definitive diagnosis of TBM (as even the co-occurrence of ABVIs, PAs, and APDIs (in any possible combination) can result from pathological conditions other than TBM), if ABVIs, PAs, and/or APDIs are concurrently present with GIs on the inner skull surface, their tuberculous origin is very likely.

3.2 | Case studies

3.2.1 | Terry No. 562

On the inner skull surface of Terry No. 562 (17-year-old, female, died of pulmonary TB), two different endocranial alteration types indicative of TBM were observed (Table 4). Multifocal GIs were registered on the orbital part of the frontal bone (Figure 2a,b), on the squamous (Figure 2c) and petrous (Figure 2d) parts of the right temporal bone, and on the squamous part of the occipital bone (Figure 2e). In addition, unifocal GIs were noted on the squamous part of the left

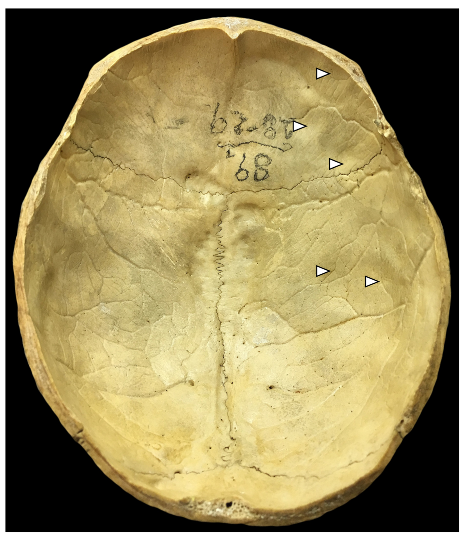

FIGURE 3 APDIs (white arrows) on the left and right parietal bones and on the squamous part of the frontal bone of Terry No. 562 (17-year-old, female, died of pulmonary TB) [Colour figure can be viewed at wileyonlinelibrary.com]

temporal bone and on the right greater wing of the sphenoid bone (Figure 2c). In the occipital and right temporal bones, GIs covered about one-third of the endocranial surfaces; whereas in the frontal, left temporal, and sphenoid bones, the observed lesions affected only a small proportion of the inner surfaces. Besides GIs, slightly pronounced APDIs, affecting the left and right parietal bones and the squamous part of the frontal bone, were recorded (Figure 3).

In the postcranial skeleton of Terry No. 562, the ribs and spine revealed bony changes that can presumably be attributed to TB (Table 4). Five left side ribs (2nd–6th) showed slight PNBFs on the visceral surface of the vertebral and sternal ends. In the vertebral column, signs of hypervascularization were registered in the form of circumferential pitting on the lateral aspects of the lower thoracic (T9–12) and lumbar (L1–5) vertebral bodies.

3.2.2 | Terry No. 933R

On the inner skull surface of Terry No. 933R (40-year-old, male, died of peritoneal TB without involvement of the lungs), three types of endocranial bony changes probably resulted from TBM were noted (Table 4). The squamous (Figure 4a,b,d) and orbital (Figure 4c) parts of the frontal bone, the left and right parietal bones (along the squamous suture), and the squamous part of the occipital bone (Figure 5c) revealed multifocal GIs. The squamous part of the left (Figure 5a) and right temporal bones, and the left (Figure 5b) and right greater wings of the sphenoid bone displayed unifocal GIs. Except for the occipital bone, the extent of the observed GIs did not exceed one-third of the endocranial surface on the affected cranial bones. Besides GIs, multifocal, small, serpentine branching ABVIs were detected on the squamous part of the frontal bone (Figure 4a), covering about one-third of the inner surface. Moreover, shallow APDIs were also recorded on the squamous part of the frontal bone (Figure 4a), representing the very slight prominence stage.

In the postcranial skeleton of Terry No. 933R, the spine and a rib exhibited bony changes likely associated with TB (Table 4). The vertebral column showed signs of hypervascularization in the form of multiple, circumferential, smooth-walled resorptive pits occasionally connected by horizontal, superficial vascular impressions on the lateral and anterior aspects of the lower cervical (C6–7) and thoracic (T1–12) vertebral bodies, as well as on the lateral aspects of the upper lumbar (L1–2) vertebral bodies. Furthermore, PNBFs were noted on the visceral surface of the body of the 11th right side rib.

3.2.3 | Terry No. 1159

On the inner skull surface of Terry No. 1159 (26-year-old, male, died of pulmonary TB), three types of pathological bony changes indicative

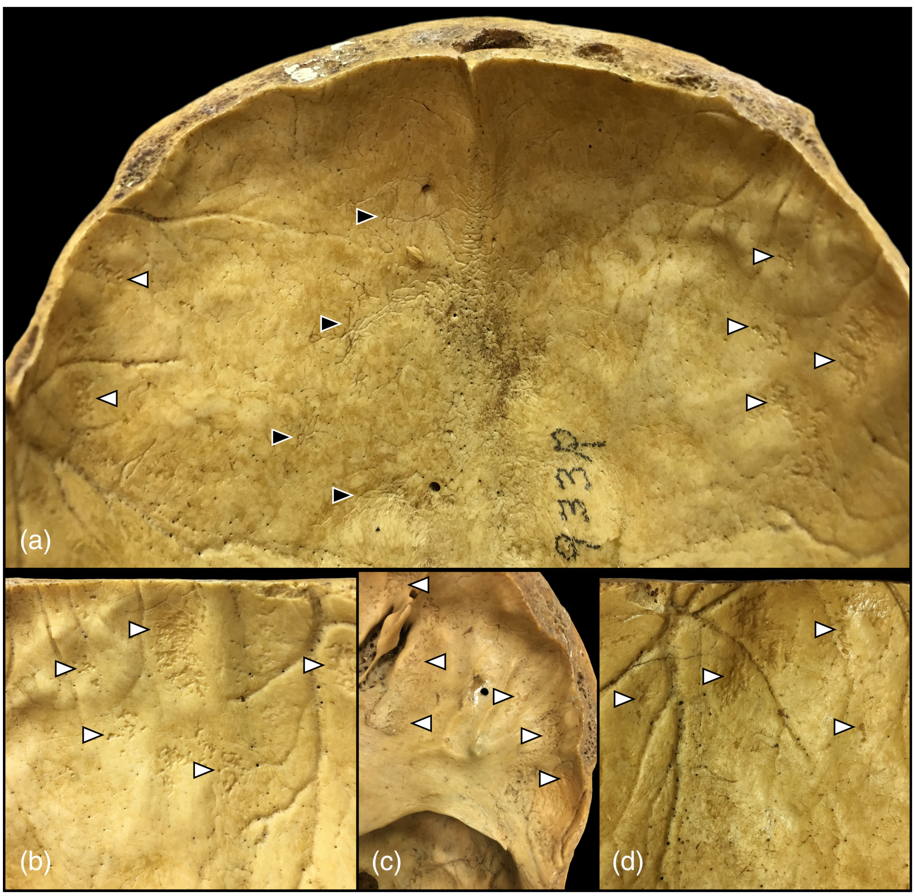

FIGURE 4 GIs (white arrows), ABVIs (black arrows), and APDIs on (a) the squamous part of the frontal bone of Terry No. 933R (40-year-old, male, probably died of peritoneal TB without involvement of the lungs); and GIs (white arrows) on the frontal bone of Terry No. 933R (40-year-old, male, probably died of peritoneal TB without involvement of the lungs): (b) left side of the squamous part, (c) orbital part, and (d) right side of the squamous part [Colour figure can be viewed at wileyonlinelibrary.com]

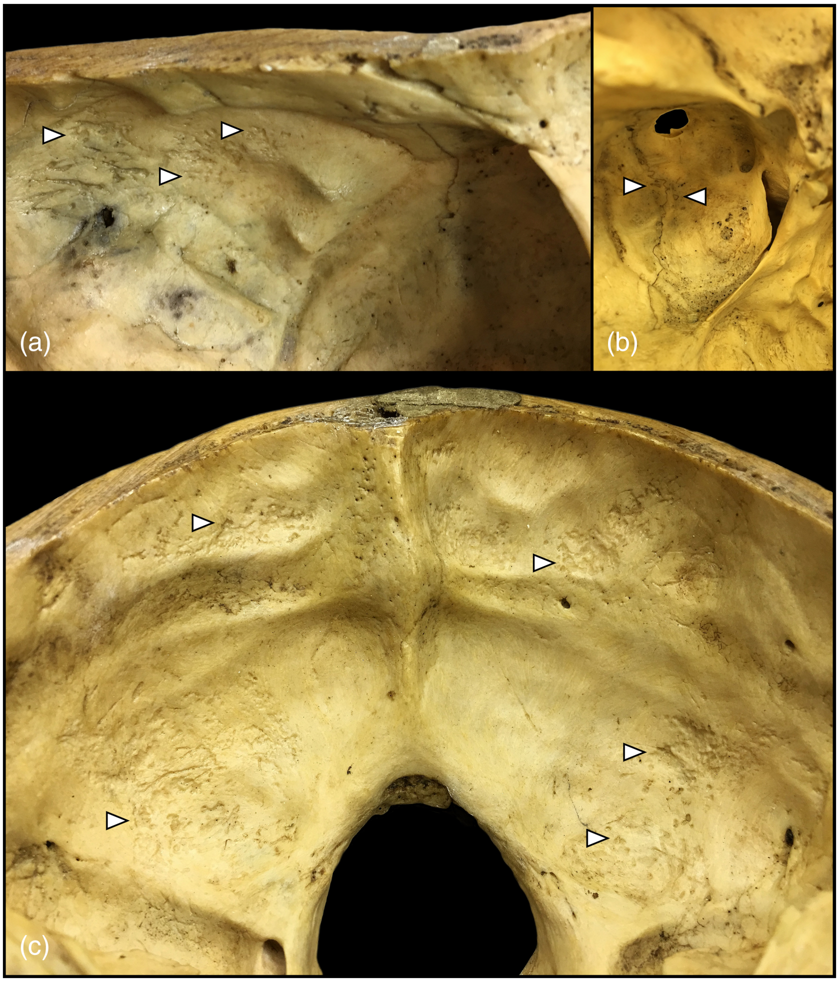

FIGURE 5 GIs (white arrows) on (a) the squamous part of the left temporal bone, (b) the left greater wing of the sphenoid bone, and (c) the squamous part of the occipital bone of Terry No. 933R (40-year-old, male, probably died of peritoneal TB without involvement of the lungs) [Colour figure can be viewed at wileyonlinelibrary.com]

of TBM were registered (Table 4). Multifocal GIs were recorded on the orbital part of the frontal bone (Figure 6) and on the squamous part of the occipital bone. The observed GIs covered less than one-fourth of the endocranial surface in both cranial bones affected. Multifocal, small patches of PAs were detected on the squamous (Figures 7a and 8b) and orbital (Figures 6 and 8a) parts of the frontal bone, along the sagittal suture on the left and right parietal bones (Figures 7c and 8b), and on the squamous part of the temporal (Figure 7b) and occipital bones. The extent of the observed PAs did not exceed one-fourth of the affected endocranial surfaces. Moreover, shallow, slightly pronounced APDIs were noted all over the inner surface of the skullcap (Figure 8a) and skull base (Figure 8b).

Similar to the skull, the postcranial skeleton of Terry No. 1159 also exhibited different types of bony changes that are suggestive of TB (Table 4). Ten left side ribs (second to 11th) showed very slight PNBFs on the visceral surface of the vertebral end (second to fourth and eighth to ninth), body (second to third, sixth, and ninth to 11th), and sternal end (second to 10th). Besides the ribs, the lateral and posterior surfaces of both tibiae (predominantly the proximal portion of the shaft), the anterior surface of both humeri (particularly the distal portion of the shaft), and the supraspinatous fossa of the right scapula also revealed slight PNBFs. The spine displayed signs of hypervascularization in form of circumferential pitting on the anterior

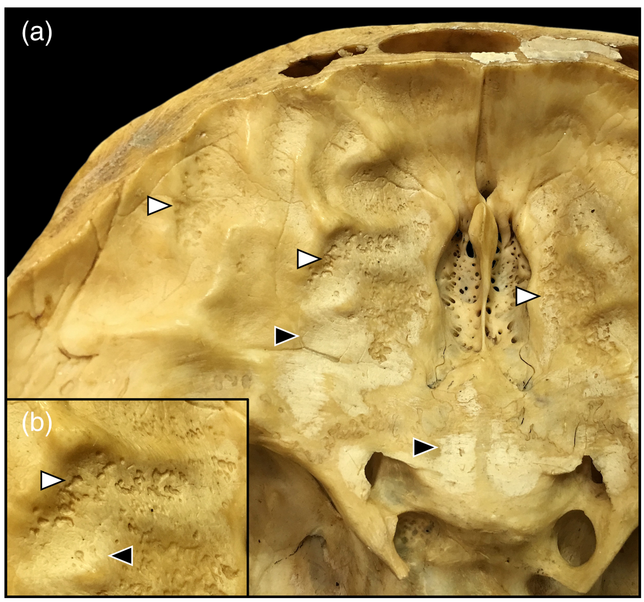

FIGURE 6 (a) GIs (white arrows) and PAs (black arrows) on the orbital part of the frontal bone of Terry No. 1159 (26-year-old, male, died of pulmonary TB); and (b) close-up of GIs (white arrows) and PAs (black arrows) on the orbital part of the frontal bone of Terry No. 1159 (26-year-old, male, died of pulmonary TB) [Colour figure can be viewed at wileyonlinelibrary.com]

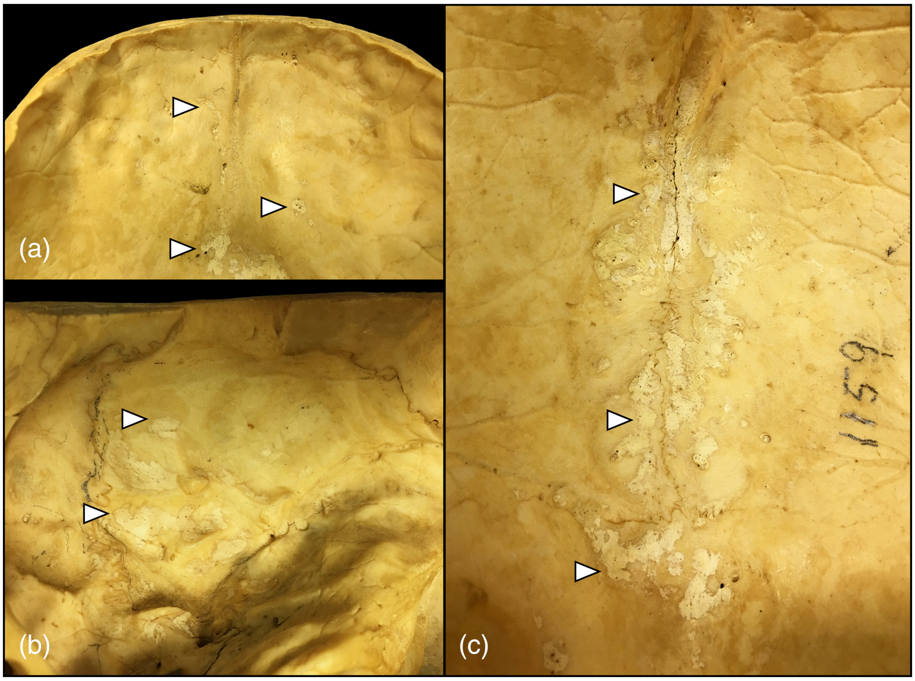

FIGURE 7 PAs (white arrows) on (a) the squamous part of the frontal bone, (b) the squamous part of the right temporal bone, and (c) the left and right parietal bones (along the sagittal suture) of Terry No. 1159 (26-year-old, male, died of pulmonary TB) [Colour figure can be viewed at wileyonlinelibrary.com]

aspect of the upper thoracic (T1–4) and on the lateral aspects of the middle and lower thoracic (T5–12), and upper lumbar (L1–3) vertebral bodies.

In summary, during the macromorphological evaluation of the three selected skeletons from the Terry Collection, GIs and APDIs were detected in all of them, whereas ABVIs and PAs were noted in Terry No. 933R and Terry No. 1159, respectively (Table 4). Although ABVIs, PAs, and APDIs cannot be considered as pathognomonic features of TBM, their co-occurrence with GIs strengthens their tuberculous origin in the three demonstrated cases.

As for the non-endocranial bony changes, costal PNBFs and vertebral hypervascularization were recorded in all the three selected individuals (Table 4). PNBFs on the visceral rib surface were associated with pulmonary TB/TB pleurisy following examination of skeletons of known cause of death from documented anatomical collections (e.g., Terry Collection and Coimbra Identified Skeletal Collection), as they occurred more frequently in individuals recorded to have died of TB than in those identified to have died of non-TB causes (e.g., Giacon, 2008; Kelley & Micozzi, 1984; Maczel, 2003; Matos & Santos, 2006; Roberts et al., 1994; Santos & Roberts, 2001, 2006). Pulmonary TB can provoke a localized or generalized inflammatory response on the visceral costal surfaces (i.e., the formation of PNBFs) by initiating the development of TB pleurisy. Nevertheless, several pulmonary diseases other than TB, as well as non-pulmonary ones (e.g., acute lobar pneumonia, bronchiectasis, metastatic carcinoma, pyogenic osteomyelitis, and actinomycosis), can also stimulate the formation of PNBFs on the inner surface of ribs (Matos & Santos, 2006; Roberts et al., 1994; Santos & Roberts, 2001, 2006).

Vertebral hypervascularization, in form of circumferential, multiple, smooth-walled resorptive pits that are often connected by horizontal, superficial vascular impressions on the anterior and/or lateral aspects of the thoracic and lumbar vertebral bodies, was described as a probable sign of early-stage skeletal TB in several paleopathological studies on osteoarchaeological series and documented anatomical collections (e.g., Baker, 1999; Giacon, 2008; Maczel, 2003; Mariotti et al., 2015; Ménard, 1888; Pálfi et al., 2012). Although, similar to costal PNBFs, vertebral hypervascularization can be of tuberculous origin, it is not specific to the disease.

Besides costal PNBFs and signs of vertebral hypervascularization, PNBFs were observed on the shaft of several long tubular bones of Terry No. 1159 (Table 4). Diffuse, bilateral, symmetrical PNBFs predominantly affecting the distal and periarticular parts of the shaft of short and/or long tubular bones are characteristic features of hypertrophic pulmonary osteopathy (HPO). Although the etiology of HPO is still unknown, the secondary form of the disease was often associated with pulmonary TB in both paleopathological and contemporary clinical studies (e.g., Assis et al., 2011; Hershkovitz et al., 2002; Kelly et al., 1991; Masson et al., 2013; Winland et al., 1997; Yap et al., 2017)—nevertheless, other pulmonary (e.g., lung cancer), as well as non-pulmonary (e.g., inflammatory bowel disease and cirrhosis) conditions can also result in the development of HPO.

It should be noted that the aforementioned non-endocranial alterations registered in the skeleton of Terry No. 562, Terry No. 933R, and Terry No. 1159 cannot be considered as pathognomonic signs of TB. Nonetheless, their co-occurrence with GIs (and the three other endocranial alteration types indicative of TBM), as well as the recorded cause of death of the examined individuals (i.e., pulmonary TB and peritoneal TB) constitute evidence that they are very likely of tuberculous origin in the three presented cases from the Terry Collection.

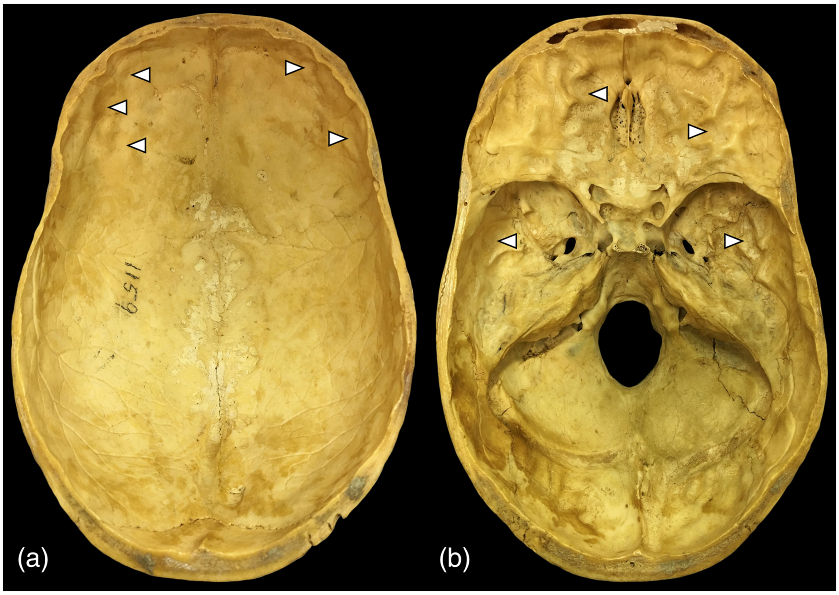

FIGURE 8 APDIs (white arrows) all over the inner surface of the (a) skullcap and (b) skull base of Terry No. 1159 (26-year-old, male, died of pulmonary TB) [Colour figure can be viewed at wileyonlinelibrary.com]

4 | CONCLUSIONS

The statistical findings of the current paper strengthen the paleopathological diagnostic value of GIs, ABVIs, PAs, and APDIs. Based on the calculated sensitivity and specificity estimate values, there is a positive association between TB and the four aforementioned lesion types; therefore, all of them can be used as paleopathological diagnostic criteria for the disease. GIs, which are pathognomonic for TBM, are sufficient enough on their own to make a definitive diagnosis of the disease, whereas ABVIs, PAs, and APDIs are not specific to TBM but can be of tuberculous origin. Although ABVIs, PAs, and APDIs (or even their co-occurrence in any possible combination) are not suitable on their own to identify individual TBM cases in past human populations, they can still be used as diagnostic criteria for the disease, especially in paleoepidemiological studies where the main aim is not to identify individual cases of TB but to estimate the prevalence of the disease in a given osteoarchaeological series (Boldsen, 2001; Dangvard Pedersen et al., 2019; Milner & Boldsen, 2017).

Furthermore, the three example cases from the Terry Collection (i.e., Terry No. 562, Terry No. 933R, and Terry No. 1159) that were demonstrated in detail in the current paper provide paleopathologists with a stronger basis for identifying TBM in ancient human remains that reveal endocranial alterations resembling that of the presented cases, as these three skeletons exhibit bony changes on the inner skull surface that are representative of the macromorphological appearance (e.g., localization) and co-occurrence of GIs, ABVIs, PAs, and APDIs (in different combinations). It should be mentioned that the current study has a major limitation—during the investigations in the Terry Collection, only macroscopic evaluation could be performed on the three selected skeletons. Nevertheless, in the future, by applying not only macromorphological methods but also imaging (e.g., micro-CT) and/or microscopy (e.g., polarized light microscopy) techniques, we can get a better insight into the morphological appearance of GIs, ABVIs, PAs, and APDIs observed in the three demonstrated cases from the Terry Collection and further strengthen their supposed etiology.

ACKNOWLEDGMENTS

Funding provided by the University of Szeged Open Access Fund (5626), the Hungarian State Eötvös Fellowship 2016 (77466) of the Tempus Public Foundation, the NTP-NFTÖ-16 (1116) of the Hungarian Ministry of Human Capacities & Human Capacities Grant Management Office, and the National Research, Development and Innovation Office, Hungary (K 125561) is greatly acknowledged.

ORCID

Olga Spekker https://orcid.org/0000-0002-0350-1906
William Berthon https://orcid.org/0000-0003-1776-4798

REFERENCES

Abegg, C., Dutour, O., Desideri, J., & Besse, M. (2020). Cases of *serpens endocrania symmetrica* in young individuals from Neolithic Western Switzerland: Description and interpretation. *International Journal of Osteoarchaeology*, *30*(3), 401–409. https://doi.org/10.1002/oa.2863

Assis, S., Santos, A. L., & Roberts, C. A. (2011). Evidence of hypertrophic osteoarthropathy in individuals from the Coimbra Skeletal Identified Collection (Portugal). *International Journal of Paleopathology*, *1*(3–4), 155–163. https://doi.org/10.1016/j.ijpp.2012.02.009

Baker, B. J. (1999). Early manifestations of tuberculosis in the skeleton. In G. Pálfi, O. Dutour, J. Deák, & I. Hutás (Eds.), *Tuberculosis: Past and present* (pp. 301–307). TB Foundation: Szeged, Hungary & Golden Book Publisher.

Bell, W. E. (1978). Increased intracranial pressure—Diagnosis and management. *Current Problems in Pediatric and Adolescent Health Care*, *8*(4), 1–62. https://doi.org/10.1016/S0045-9380(78)80005-X

Boldsen, J. L. (2001). Epidemiological approach to the paleopathological diagnosis of leprosy. *American Journal of Physical Anthropology*, *115*(4), 380–387. https://doi.org/10.1002/ajpa.1094

Burkhardt, L., & Fischer, H. (1970). Pathologische Anatomie des Schädels. In E. Uehlinger (Ed.), *Handbuch der speziellen pathologischen Anatomie und Histologie, volume 9, part 7* (pp. 1–352). Springer Verlag.

Dangvard Pedersen, D., Milner, G. R., Kolmos, H. J., & Boldsen, J. L. (2019). The association between skeletal lesions and tuberculosis diagnosis using a probabilistic approach. *International Journal of Paleopathology*, *27*, 88–100. https://doi.org/10.1016/j.ijpp.2019.01.001

Desai, V., Priyadarshini, S. R., & Sharma, R. (2014). Copper beaten skull! Can it be a usual appearance? *International Journal of Clinical Pediatric Dentistry*, *7*(1), 47–49. https://doi.org/10.5005/jp-journals-10005-1233

du Boulay, G. H. (1956). The significance of digital impressions in children's skulls. *Acta Radiologica*, *46*(1–2), 112–122. https://doi.org/10.3109/00016925609170820

Giacon, M. (2008). *Paleopathology in the osteological collection of Anthropological Museum in Padova University: The cases of tuberculosis*. PhD Dissertation, Padova University.

Hershkovitz, I., Greenwald, C. M., Latimer, B., Jellema, L. M., Wish-Baratz, S., Eshed, V., Dutour, O., & Rotschild, B. M. (2002). *Serpens endocrania symmetrica* (SES): A new term and a possible clue for identifying intrathoracic disease in skeletal populations. *American Journal of Physical Anthropology*, *118*(3), 201–216. https://doi.org/10.1002/ajpa.10077

Jankauskas, R. (1999). Tuberculosis in Lithuania: Paleopathological and historical correlations. In G. Pálfi, O. Dutour, J. Deák, & I. Hutás (Eds.), *Tuberculosis: Past and present* (pp. 549–558). TB Foundation: Szeged, Hungary & Golden Book Publisher.

Janovic, A., Milovanovic, P., Sopta, J., Rakocevic, Z., Filipovic, V., Nenezic, D., & Djuric, M. (2015). Intracranial arteriovenous malformations as a possible cause of endocranial bone lesions and associated neurological disorder. *International Journal of Osteoarchaeology*, *25*(1), 88–97. https://doi.org/10.1002/oa.2266

Kelley, M. A., & Micozzi, M. S. (1984). Rib lesions in chronic pulmonary tuberculosis. *American Journal of Physical Anthropology*, *65*(4), 381–386. https://doi.org/10.1002/ajpa.1330650407

Kelly, P., Manning, P., Corcoran, P., & Clancy, L. (1991). Hypertrophic osteoarthropathy in association with pulmonary tuberculosis. *Chest*, *99*(3), 769–770. https://doi.org/10.1378/chest.99.3.769

Lei, S., Pechenkina, K., Yanpeng, C., Hai, Z., & Xueyi, Q. (2019). Cases of endocranial lesions on juvenile skeletons from Longshan cultural sites in Henan Province, China. *International Journal of Paleopathology*, *26*, 61–74. https://doi.org/10.1016/j.ijpp.2019.06.001

Lewis, M. E. (2004). Endocranial lesions in non-adult skeletons: Understanding their aetiology. *International Journal of Osteoarchaeology*, *14*(2), 82–97. https://doi.org/10.1002/oa.713

Maczel, M. (2003). *"On the traces of tuberculosis" Diagnostic criteria of tuberculosis affection of the human skeleton and their application in Hungarian and French anthropological series*. PhD dissertation. University of La Méditerranée – Aix Marseille II Faculty of Medicine: Marseille, France & University of Szeged, Faculty of Science.

Mahomed, N., Sewchuran, T., & Mahomed, Z. (2012). The copper-beaten skull. *South African Journal of Radiology*, *16*(1), 25–26. https://doi.org/10.4102/sajr.v16i1.229

Mariotti, V., Zuppello, M., Pedrosi, M. E., Bettuzzi, M., Brancaccio, R., Peccenini, E., Morigi, M. P., & Belcastro, M. G. (2015). Skeletal evidence of tuberculosis in a modern identified human skeletal collection (Certosa cemetery, Bologna, Italy). *American Journal of Physical Anthropology*, *157*(3), 389–401. https://doi.org/10.1002/ajpa.22727

Masson, M., Molnár, E., Donoghue, H. D., Besra, G. S., Minnikin, D. E., Wu, H. H. T., Lee, O. Y.-C., Bull, I. D., & Gy, P. (2013). Osteological and biomolecular evidence of a 7000-year-old case of hypertrophic pulmonary osteopathy secondary to tuberculosis from Neolithic Hungary. *PLoS ONE*, *8*(10), e78252. https://doi.org/10.1371/journal.phone.0078252

Matos, V., & Santos, A. L. (2006). On the trail of pulmonary tuberculosis based on rib lesions: Results from the human identified skeletal collection from the Museu Bocage (Lisbon, Portugal). *American Journal of Physical Anthropology*, *130*(2), 190–200. https://doi.org/10.1002/ajpa.20309

Ménard, V. (1888). *Tuberculose vertébrale*. Paris, France.

Milner, G. R., & Boldsen, J. L. (2017). Life not death: Epidemiology from skeletons. *International Journal of Paleopathology*, *17*, 26–39. https://doi.org/10.1016/j.ijpp.2017.03.007

Myers, J. N. (2007). Miliary, central nervous system, and genitourinary tuberculosis. *Disease-a-Month*, *53*(1), 22–31. https://doi.org/10.1016/j.disamonth.2006.10.003

Ortner, D. J. (2003). Infectious diseases: Tuberculosis and leprosy. In D. J. Ortner (Ed.), *Identification of pathological conditions in human skeletal remains* (pp. 227–271). Academic Press. https://doi.org/10.1016/B978-012528628-2/50047-8

Pálfi, G., Bereczki, Z., Ortner, D. J., & Dutour, O. (2012). Juvenile cases of skeletal tuberculosis from the Terry Anatomical Collection (Smithsonian Institution, Washington, DC, USA). *Acta Biologica Szegediensis*, *56*(1), 1–12.

Paul, S., Smith, J., Green, J., Smith-Collins, A., & Chinthapalli, R. (2013). Managing children with raised intracranial pressure: Part one (introduction and meningitis). *Nursing Children and Young People*, *25*(10), 31–36. https://doi.org/10.7748/ncyp2013.12.25.10.31.e214

Paul, S., Smith, J., Green, J., Smith-Collins, A., & Chinthapalli, R. (2014). Managing children with raised intracranial pressure: Part two (brain tumours and intracranial bleeds). *Nursing Children and Young People*, *26*(1), 30–37. https://doi.org/10.7748/ncyp2014.02.26.1.30.e214

Pemmaiah, D. C. (2015). Copper beaten skull. *Journal of Medical Sciences and Health*, *1*(2), 46–48.

Roberts, C. A., Lucy, D., & Manchester, K. (1994). Inflammatory lesions of ribs: An analysis of the Terry collection. *American Journal of Physical Anthropology*, *95*(2), 169–182. https://doi.org/10.1002/ajpa.1330950205

Roberts, C. A., Pfister, L.-A., & Mays, S. (2009). Letter to the editor: Was tuberculosis present in *Homo erectus* in Turkey? *American Journal of Physical Anthropology*, *139*(3), 442–444. https://doi.org/10.1002/ajpa.21056

Santos, A. L., & Roberts, C. A. (2001). A picture of tuberculosis in young Portuguese people in the early 20th century: A multidisciplinary study of the skeletal and historical evidence. *American Journal of Physical Anthropology*, *115*(1), 38–49. https://doi.org/10.1002/ajpa.1054

Santos, A. L., & Roberts, C. A. (2006). Anatomy of a serial killer: Differential diagnosis of tuberculosis based on rib lesions of adult individuals from the Coimbra Identified Skeletal Collection, Portugal. *American Journal of Physical Anthropology*, *130*(1), 38–49. https://doi.org/10.1002/ajpa.20160

Schüller, A. (1940–1941). X-ray symptoms of intracranial hypertension. *Confinia Neurologica*, *3*(1–2), 253–256. https://doi.org/10.1159/000106215

Schultz, M. (1993). *Spuren unspezifischer Entzündungen an prähistorischen und historischen Schädeln. Ein Beitrag zur Paläopathologie*. Anthropologisches Forschungsinstitut: Aesch, Switzerland & Anthropologische Gesellschaft.

Schultz, M. (1999). The role of tuberculosis in infancy and childhood in prehistoric and historic populations. In G. Pálfi, O. Dutour, J. Deák, & I. Hutás (Eds.), *Tuberculosis: Past and present* (pp. 503–507). TB Foundation: Szeged, Hungary & Golden Book Publisher.

Schultz, M. (2001). Paleohistopathology of bone: A new approach to the study of ancient diseases. *American Journal of Physical Anthropology*, *116*(Suppl. 33), 106–147. https://doi.org/10.1002/ajpa.10024

Schultz, M. (2003). Light microscopic analysis in skeletal paleopathology. In D. J. Ortner (Ed.), *Identification of pathological conditions in human skeletal remains* (pp. 73–107). Academic Press. https://doi.org/10.1016/B978-012528628-2/50043-0

Schultz, M., & Schmidt-Schultz, T. H. (2015). Is it possible to diagnose TB in ancient bone using microscopy? *Tuberculosis*, *95*(Suppl. 1), S80–S86. https://doi.org/10.1016/j.tube.2015.02.035

Spekker, O. (2018). Evaluation of endocranial bony changes in relation to tuberculosis in the Robert J. Terry Anatomical Skeletal Collection (Washington, DC, USA). PhD Dissertation, University of Szeged: Szeged, Hungary. https://doi.org/10.14232/phd.9714

Spekker, O., Hunt, D. R., Berthon, W., Paja, L., Molnár, E., Gy, P., & Schultz, M. (2021). Tracking down the White Plague. Chapter three: Revision of endocranial abnormally pronounced digital impressions as paleopathological diagnostic criteria for tuberculous meningitis. *PLoS ONE*, *16*(3), e0249020. https://doi.org/10.1371/journal.pone.0249020

Spekker, O., Hunt, D. R., Paja, L., Molnár, E., Gy, P., & Schultz, M. (2020). Tracking down the White Plague: The skeletal evidence of tuberculous meningitis in the Robert J. Terry Anatomical Skeletal Collection. *PLoS ONE*, *15*(3), e0230418. https://doi.org/10.1371/journal.pone.0230418

Spekker, O., Schultz, M., Paja, L., Váradi, O. A., Molnár, E., Gy, P., & Hunt, D. R. (2020). Tracking down the White Plague. Chapter two: The role of endocranial abnormal blood vessel impressions and periosteal appositions in the paleopathological diagnosis of tuberculous meningitis. *PLoS ONE*, *15*(9), e0238444. https://doi.org/10.1371/journal.pone.0238444

Teschler-Nicola, M., Novotny, F., Spannagl-Steiner, M., Stadler, P., Prohaska, T., Irrgeher, J., Zitek, A., Däubl, B., Haring, E., Rumpelmayr, K., & Wild, E. M. (2015). The early medieval manorial estate of Gars/Thunau, Lower Austria: An enclave of endemic tuberculosis? *Tuberculosis*, *95*(Suppl. 1), S51–S59. https://doi.org/10.1016/j.tube.2015.02.017

Winland, K., Rothschild, B. M., & Rothschild, C. (1997). Reproducibility of patterns of tuberculosis-related periosteal reaction in the Hamman-Todd, Grant & Terry Collections. *American Journal of Physical Anthropology*, *24*, 243.

Yap, F. Y., Skalski, M. R., Patel, D. B., Schein, A. J., White, E. A., Tomasian, A., Masih, S., & Matcuk, G. R. (2017). Hypertrophic osteoarthropathy: Clinical and imaging features. *Radiographics*, *37*(1), 157–175. https://doi.org/10.1148/rg.2017160052

SUPPORTING INFORMATION

Additional supporting information may be found in the online version of the article at the publisher's website.

How to cite this article: Spekker, O., Hunt, D. R., Berthon, W., Molnár, E., & Pálfi, G. (2022). Insights into the diagnostic efficacy and macroscopic appearance of endocranial bony changes indicative of tuberculous meningitis: Three example cases from the Robert J. Terry Anatomical Skeletal Collection. *International Journal of Osteoarchaeology*, *32*(2), 444–456. https://doi.org/10.1002/oa.3079